Available online at www.sciencedirect.com
ScienceDirect
Catalysis Today 128 (2007) 36–46
CATALYSIS TODAY
www.elsevier.com/locate/cattod

Kinetic and selectivity studies of gas–liquid reaction under Taylor flow in a circular capillary

A.N. Tsoligkas [a], M.J.H. Simmons [a], J. Wood [a,*], C.G. Frost [b]

[a] *Centre for Formulation Engineering, Department of Chemical Engineering, University of Birmingham, Edgbaston, Birmingham B15 2TT, UK*
[b] *Department of Chemistry, University of Bath, Bath BA2 7AY, UK*

Available online 14 August 2007

Abstract

The catalytic hydrogenation of 2-butyne-1,4-diol to *cis*-2-butene-1,4-diol and butane-1,4-diol was carried out in a circular capillary operating in co-current down-flow mode in order to mimic the behaviour of a monolith channel. The selected model reaction was performed over a 4 wt.% palladium/alumina catalyst using 30% (v/v) isopropanol/water solvent. Liquid and gas superficial velocities were varied over a wide range ($0.0098 < V_{SG} < 0.0356$ m s^{-1} and $0.0074 < V_{SL} < 0.1485$ m s^{-1}) in order to study the effect of gas bubble and liquid slug lengths on the observed reaction rate and selectivity towards *cis*-2-butene-1,4-diol. At constant V_{SG}, upon increasing V_{SL} the reaction rate was sensitive to liquid slug length (L_S) and flow pattern such that the maximum reaction rate occurred at $L_S/D = 1.2$. While at constant V_{SL}, upon increasing V_{SG} the reaction rate was influenced by both gas (L_G) and liquid slug lengths, decreasing from 0.0012 mol l^{-1} min^{-1} to reach a steady value. Varying the liquid slug length caused the selectivity to increase from 20 to 88%, whilst varying the gas slug length had a smaller effect, whereupon the selectivity slightly decreased from 95 to 83.6%. A model was developed to predict the concentration profiles of reactants and products incorporating a Langmuir–Hinshelwood model of the kinetics and correlations for estimating mass transfer coefficients from the literature.

Keywords: Multiphase reactions; Mass transfer; Capillary; Selectivity; Hydrodynamics

1. Introduction

Monolith structures were originally designed for single-phase reactions, particularly in automotive exhaust catalysis and in the treatment of flue gas from power plants. Over the past decade, following successful utilisation of monolith reactors for gas phase reactions, an increased amount of research has been carried out using monoliths for catalysed multiphase gas–liquid reactions. Comparison of the performance of monolith reactors with other more traditional types of reactor including mechanically agitated slurry reactors [1] or trickle bed reactors [2–6] have shown that the monolith reactor configuration has several unique advantages which give superior performance, e.g. low pressure drop, high geometric surface area, high resistance to blockage, high selectivity, high productivity and high mass transfer rates. Irrespective of many advantages over other types of multiphase reactors, there is only one example of commercial application of monolithic catalysts in multiphase processes. Akzo–Nobel operates a monolith reactor for the production of hydrogen peroxide in a large scale using the anthraquinone autoxidation process [7,8]. Early studies of flow in monoliths operating as multiphase systems showed that maldistribution of gas and liquid across the channels could occur. For example magnetic resonance imaging (MRI) was used [9] to observe irregularities of gas and liquid lengths and bubble velocities in a co-current down-flow bubble column reactor. However, recent studies focussing on the stability of Taylor flow [10,11] have led to the development of a model based on the two phase pressure gradient which enables prediction of both stable and unstable regimes in the monolith reactor. The model also incorporates the two-phase velocity of downward Taylor flow when the pressure gradient over the column is zero: termed the free velocity.

A considerable number of different gas–liquid–solid catalytic reactions have been tested using monolith catalyst supports as a means of assessing their possible application, for example hydrogenation reactions [12,5], photocatalytic oxidations [13]

* Corresponding author.

0920-5861/$ – see front matter © 2007 Elsevier B.V. All rights reserved.
doi:10.1016/j.cattod.2007.07.001

Nomenclature

a	interface area ($m^2\ m^{-3}$)
C	concentration ($mol\ l^{-1}$)
C^*	saturated concentration ($mol\ l^{-1}$)
D	diameter of the channel (mm)
D_i	diffusion coefficient of diffusing component in the liquid ($m^2\ s^{-1}$)
k	mass transfer coefficient ($m\ s^{-1}$)
k_r	reaction rate constant ($kmol\ m^{-3}\ s^{-1}$)
K	adsorption coefficient ($m^3\ kmol^{-1}$)
L_G	gas length (mm)
L_S	liquid length (mm)
R	modelled reaction rate ($mol\ l^{-1}\ min^{-1}$)
R_1	observed reaction rate ($mol\ l^{-1}\ min^{-1}$)
R_2	reaction rate described by a Langmuir–Hinshelwood (L–H) type relationship ($mol\ l^{-1}\ min^{-1}$)

Greek letters

δ	liquid film thickness (m)
ε_L	liquid fraction in the capillary

Subscripts/superscripts

B1	butane-1,4-diol
B2	2-butene-1,4-diol
B3	2-butyne-1,4-diol
B3,b	bulk concentration of 2-butyne-1,4-diol
B3I	2-butyne-1,4-diol initial concentration
G	gas phase
GL	gas–liquid
GS	gas–solid
H_2S	hydrogen at surface
L	liquid phase
LS	liquid–solid
S	superficial

and biochemical applications [14]. However, due to the possibility of several side reactions, it is important to optimise the reactor operating conditions to maximise the selectivity towards the desired product and thus reduce waste of the reagents. In this study the selective hydrogenation of 2-butyne-1,4-diol towards *cis*-2-butene-1,4-diol is used as the model reaction since selective hydrogenations with an intermediate being the desired product are typical in chemical industries. For example, from previous studies [15], the selectivity towards *cis*-2-butene-1,4-diol in the hydrogenation of 2-butyne-1,4-diol was found to be a function of catalyst loading, temperature, solvent, base addition, metal additives and the support material. 2-Butene-1,4-diol is an important chemical intermediate for the manufacture of endosulfan—an insecticide [16] and vitamins A and B6. 2-Butene-1,4-diol is obtained commercially via selective hydrogenation of 2-butyne-1,4-diol. The hydrogenation of 2-butyne1-,4-diol results in two main products, 2-butene-1,4-diol (*cis* and *trans* isomers) and butane-1,4-diol, together with a number of side products such as γ-hydroxy butyraldehyde, *n*-butyraldehyde, *n*-butanol, crotyl alcohol and acetal as shown in Fig. 1.

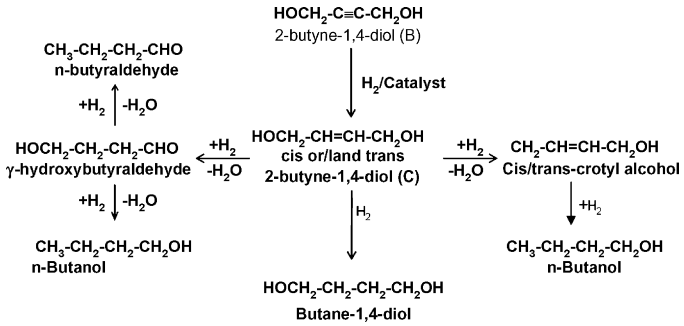

Fig. 1. The reaction network for 2-butyne-1,4-diol hydrogenation.

The aim of the work presented in this paper is to study a reaction comprised of two consecutive hydrogenation steps in a capillary reactor in order to mimic the behaviour of a monolithic reactor, which is typical for fine chemical synthesis. In a related study [17], a reaction with fast kinetics was selected, namely the catalytic hydrogenation of nitrobenzoic acid (NBA) to aminobenzoic acid (AMA), which was performed in a single capillary under widely varying hydrodynamic conditions. The intrinsic reaction rate of this reaction was so high, that the external mass transfer became rate limiting. Four main flow patterns were found namely, slug (Taylor) flow, annular, bubble and churn flow in capillaries with diameter (D) equal to 1.69 mm. The results from the investigation [17] showed that Taylor flow is the optimum flow pattern with the reaction rate mainly dependent on the liquid slug length. Over the years many researchers have reported that Taylor flow enhances mass transport [18] and heat transfer [19]. Imaging of the toroidal vortex inside the liquid slug using particle image velocimetry (PIV) [20] and other observations of flow pattern have been utilised to model the heat and mass transfer process under Taylor flow [21].

The present study provides an experimental investigation of the influence of gas (V_{SG}) and liquid superficial (V_{SL}) velocities upon gas bubble length (L_G) and liquid slug length (L_S) in a single capillary reactor and their consequent effect upon the initial reaction rate. Furthermore, the effect of V_{SL} and V_{SG} on the selectivity towards 2-butene-1,4-diol has been investigated. A kinetic model has been developed and validated by comparison between the calculated and experimental results.

2. Materials and methods

The reactor used for the hydrogenation and flow visualisation experiments is shown in Fig. 2 and consists of a vertical circular alumina ceramic capillary tube (Multilab Ltd., UK) of $D = 1.69$ mm internal diameter and 300 mm length, wash-coated with a 4% Pd on alumina catalyst by Johnson Matthey. Temperature control is measured using a thermocouple placed at the capillary inlet; feedback control maintains the temperature at $25 \pm 1\ ^\circ C$ using heating tape placed around the apparatus. A glass section allows the flow pattern to be observed. The reactant is circulated through the reactor in down-flow using a non-pulsatile pump (Encynova model 16–4), then collected in a stirred glass vessel and recirculated. Hydrogen (99.995% purity, BOC, UK) is supplied via a

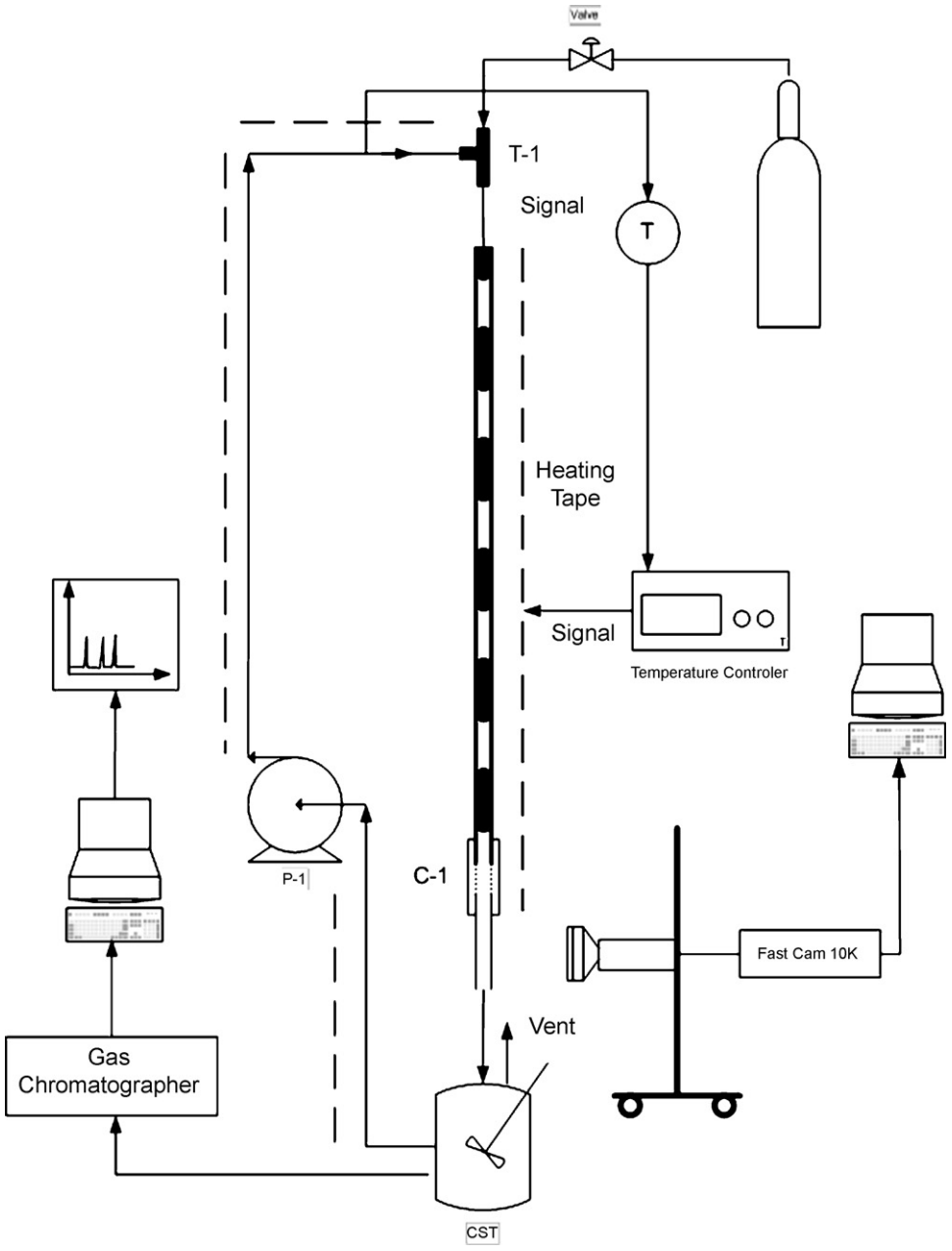

Fig. 2. Schematic diagram of the capillary reactor.

cylinder and its flow is measured using a soap film flow meter prior to the experiment.

For the reaction studies, 2-butyne-1,4-diol, (99% purity, Aldrich Chemical Company Inc.) was dissolved in 70% (v/v) water–30% (v/v) isopropanol (99.5% purity, Fisher Scientific Ltd., UK) to a concentration of 0.28 mol l^{-1}. The physical properties of the mixed solvent were $\rho = 960$ kg m^{-3}, $\sigma = 0.0275$ N m^{-1} and $\mu = 0.0023$ Pas. The experiments were performed by keeping one superficial velocity constant, whilst the other was varied. Liquid and gas superficial velocities were varied over the range $V_{SG} = 0.0098$–0.0356 m s^{-1} and $V_{SL} = 0.0074$–0.1485 m s^{-1}. The experimental conditions are listed in Table 1. The sampling was made at 30 min intervals with a total reaction time of approximately 330–450 min. The concentrations of the products and the reactants were measured using a gas chromatograph (GC, Perkin-Elmer 8700 series). The GC was fitted with a flame ionisation detector (FID) and 50 m of length, 0.32 mm I.D. CP–Wax 52 CB VARIAN capillary column with film thickness 1.2 μm. The GC output was processed using a chromatographic software CSW 32 (Data Apex Ltd., Czech Republic).

A Fastcam Super 10 K Series Model 3000 camera (Photron Ltd., UK) was used for flow visualisation and to record liquid slug lengths, L_S, and void fraction, ε_L which allowed prediction of the mass transfer coefficients [22].

3. Theory

Extensive studies have been made by numerous research groups of flow patterns in gas liquid two phase flow in

Table 1
The experimental conditions for the hydrogenation of 2-butyne-1,4-diol

Experiment	V_{SG} (m s^{-1})	V_{SL} (m s^{-1})	Initial concentration (mol l^{-1})	Temperature (°C)
1	0.0145	0.0074	0.28	24
2	0.0145	0.0223	0.28	24
3	0.0145	0.0372	0.28	24
4	0.0145	0.0743	0.28	24
5	0.0145	0.1114	0.28	24
6	0.0145	0.1485	0.28	24
7	0.0098	0.0743	0.28	24
8	0.0124	0.0743	0.28	24
9	0.0228	0.0743	0.28	24
10	0.0359	0.0743	0.28	24
11	0.0118	0.0594	0.28	24
12	0.0118	0.0594	0.28	28
13	0.0118	0.0594	0.28	30
14	0.0118	0.0594	0.28	40
15	0.0118	0.0594	0.28	45
16	0.0118	0.0594	0.28	50
17	0.0118	0.0594	0.1	24
18	0.0118	0.0594	0.18	24
19	0.0118	0.0594	0.28	24
20	0.0118	0.0594	0.42	24
21	0.0118	0.0594	0.52	24

capillaries of different diameter and orientation [23–25], using gases and liquids with different properties [24]. In the work reported here, the definition of Taylor flow is taken as a special case of slug flow with a laminar liquid phase as expressed previously [26]. The mass transfer characteristics of Taylor flow have been previously investigated [12,5,27] and it was found that hydrogen mass transport occurs in three steps. The stages are hydrogen mass transfer (i) from the gas bubble through the film surrounding the bubble to the catalyst surface (GS); (ii) transfer from the circular ends of the gas bubbles to the liquid slug (GL) and (iii) mass transfer from within the liquid slug to the channel wall (LS). Hence, considering the first stage in parallel with the second and third stages, the following relation was obtained [12]:

$$K_{OV}a = k_{GS}a_{GS} + \left(\frac{1}{k_{GL}a_{GL}} + \frac{1}{k_{LS}a_{LS}}\right)^{-1}, \quad (1)$$

where k is the mass transfer coefficient and a is the interfacial area per unit volume. This model has been used successfully [12] to predict the mass transfer rates for the hydrogenation of α-methylstyrene over a monolith catalyst and for the mass transfer limited hydrogenation of NBA in a capillary reactor [17]. Similarly, in this paper the same model is adapted for the hydrogenation of 2-butyne-1,4-diol. The mass transfer coefficients are obtained using modified relationships [22] for k_{GL} and k_{LS}, respectively:

$$k_{GL}a_{GL} = \frac{0.1111(V_{GS}+V_{LS})^{1.19}}{(\varepsilon_L UCL)^{0.57}}\left(\frac{D_{H_2}}{D_{ME}}\right)^{0.5}, \quad (2)$$

$$k_{LS}a_{LS} = \frac{0.059(V_{GS}+V_{LS})^{0.63}}{(\varepsilon_L UCL - 9.4UCL(1-\varepsilon_L)(\delta/D))^{0.41}}\left(\frac{D_{H_2}}{D_{BA}}\right)^{0.66}, \quad (3)$$

where V_{GS} and V_{LS} are the measured superficial gas and liquid velocities, δ the film thickness calculated using an empirical equation [28], L_S the liquid slug length as measured by the experiments, D_i the molecular diffusion coefficient, D_{BA} the molecular diffusion coefficient of benzoic acid, D_{ME} the molecular diffusion coefficient of methane, [29], ε_L the measured liquid volume fraction and D is the channel diameter.

More recently, computational fluid dynamic simulations [30] of the overall gas mass transfer rate under Taylor flow were compared with the equivalent experimental values [22] in 1.5 mm circular capillary diameter and a remarkably good agreement was found within 10% tolerance. Hence the mass transfer correlations are considered sufficiently reliable for use in this work.

For mass transfer across the liquid film at the sides of the gas slugs, values of $k_{GS}a_{GS}$ are obtained from film theory [12]:

$$k_{GS}a_{GS} = \frac{D_i}{\delta}\frac{4(1-\varepsilon_L)}{D}. \quad (4)$$

Three way mass transfer refers here to the combined contribution of the three mass transfer steps described above, for which the overall mass transfer coefficient, K_{OV} is found by combining Eqs. (1)–(4). Assuming the reaction rate to be equal to the rate of hydrogen mass transport, the overall rate of reaction is given by:

$$R_1 = K_{OV}a(C^*_{H_2} - C_{H_2S}), \quad (5)$$

where $C^*_{H_2}$ and C_{H_2S} are the equilibrium liquid phase hydrogen and the surface concentration of hydrogen, respectively. Since there is no means of knowing C_{H_2S}, it was calculated from Eq. (5) by taking R_1 as the experimental initial reaction rate at different initial concentrations of 2-butyne-1,4-diol (C_{B3I}). The

experimental initial reaction rate was calculated by fitting a straight line to the concentration–time curve in the range of 0–50% conversion of 2-butyne-1,4-diol and $C^*_{H_2}$ was found from previous studies on hydrogen solubility in isopropanol solvents [31].

The kinetics of the reaction may be described by a Langmuir–Hinshelwood (L–H) type relationship. A model previously applied [32] predicted rates and product distribution for monolith and capillary reactions based upon the following dual site L–H mechanism:

$$R_2 = \frac{k_r K_H C_{H_2S} K_{B3} C_{B3,b}}{\left(1 + \sqrt{K_H C_{H_2S}} + K_{B3} C_{B3,b}\right)^3}, \quad (6)$$

where k_r is the reaction rate constant, K_H and K_{B3} the adsorption coefficients, respectively for H_2 and 2-butyne-1,4-diol and $C_{B3,b}$ is the bulk concentration of the solution. For the purpose of the kinetic modelling, the trial values k_r, K_H and K_{B3} were evaluated by fitting Eq. (6) on R_1 versus C_{B3I} [5,32,33]. The L–H model, unlike the power rate law model, accounts for the adsorption of the reactants and products, where both hydrogen and 2-butyne-1,4-diol are considered to compete for the same type of sites. The half order with respect to hydrogen in Eq. (6) indicates that hydrogen dissociates upon adsorption and accounts for the simultaneous addition of two atoms of hydrogen to the alkyne. The conversion of 2-butyne-1,4-diol can be predicted from following Eq. (7)

$$-\frac{dC_{B3}}{dt} = \frac{k_r K_H C_{H_2S} K_{B3} C_{B3}}{\left(1 + \sqrt{K_H C_{H_2S}} + K_{B3} C_{B3}\right)^3}, \quad (7)$$

where C_{B3} is the concentration of 2-butyne-1,4-diol during the reaction. The material balance for 2-butene-1,4-diol is

$$-\frac{dC_{B2}}{dt} = -R_{B3} + R_{B2} = -\frac{k_r K_H C_{H_2S} K_{B3} C_{B3}}{\left(1 + \sqrt{K_H C_{H_2S}} + K_{B3} C_{B3}\right)^3} + \frac{k_{B2} C_{H_2S} C_{B2}}{\left(1 + K_{B3} C_{B3}^2\right)}, \quad (8)$$

where C_{B2} is the concentration of 2-butene-1,4-diol and k_{B2} is the rate constant for the reaction of 2-butene-1,4-diol to butane-1,4-diol. Similarly, values of k_{B2} were directly evaluated from the rate of disappearance of 2-butyne-1,4-diol from the experimental data at a given superficial velocities. The rate expression for the reaction of 2-butene-1,4-diol to butane-1,4-diol (R_{B2}) in Eq. (8) has been previously used [34] to describe the same reaction; the rate of consumption of 2-butene-1,4-diol was found to be first order with respect to the reactant. The catalytic reaction R_2 occurs at very low rates until 2-butyne-1,4-diol starts to disappear, which indicates that the adsorption of 2-butyne-1,4-diol inhibits the rate of hydrogenation of 2-butene-1,4-diol. Hence an inhibition term $(1 + K_{B3}C_{B3}^2)$ in the denominator has been incorporated in the expression for R_{B2}. The predicted butane-1,4-diol concentration (C_{B1}) was calculated from the following equation,

$$C_{B1} = C_{B3I} - C_{B3} - C_{B2}. \quad (9)$$

Solving Eqs. (7)–(9) simultaneously allowed the concentrations of all liquid phase components in the system to be calculated as a function of time.

4. Results and discussion

4.1. Effect of hydrodynamics on initial reaction rate

A typical plot of product distribution during the reaction is given in Fig. 3 for $V_{GS} = 0.013$ m s^{-1} and $V_{SL} = 0.067$ m s^{-1}. The figure shows experimental data as points and predictions from the mass transfer model as lines. The results of the model are discussed later in Section 4.2. The amount of 2-butyne-1,4-diol remaining with time followed an S-shaped profile; the rate of reaction increased and reached a maximum after approximately 180–200 min, corresponding to the steepest slope of the curve, after which the rate became almost constant until less than 5% of the 2-butyne-1,4-diol remained. Less than 1% of 2-butyne-1,4-diol was present at the end of the reaction. The predominant product formed was 2-butene-1,4-diol, which reached a maximum concentration (selectivity) of 81% after 230 min, at which time the other components in the mixture were 14% 2-butyne-1,4-diol and 6% 2-butane-1,4-diol. This behaviour may be explained as due to the effect of competitive adsorption between hydrogen and 2-butyne-1,4-diol, where at high 2-butyne-1,4-diol concentrations, most of active sites are occupied by 2-butyne-1,4-diol leaving hydrogen as a limiting reactant. After 200 min (75% consumption of 2-butyne-1,4-diol), it appears that the reaction rate became independent of 2-butyne-1,4-diol concentration: this is possibly due to more hydrogen being available on the catalyst surface.

Very little 2-butane-1,4-diol was formed until most of the 2-butyne-1,4-diol had reacted to form 2-butene-1,4-diol; its production increased rapidly by consumption of the 2-butene-1,4-diol formed after 230 min into the reaction. Other products such as crotyl alcohol and *n*-butanol were not produced.

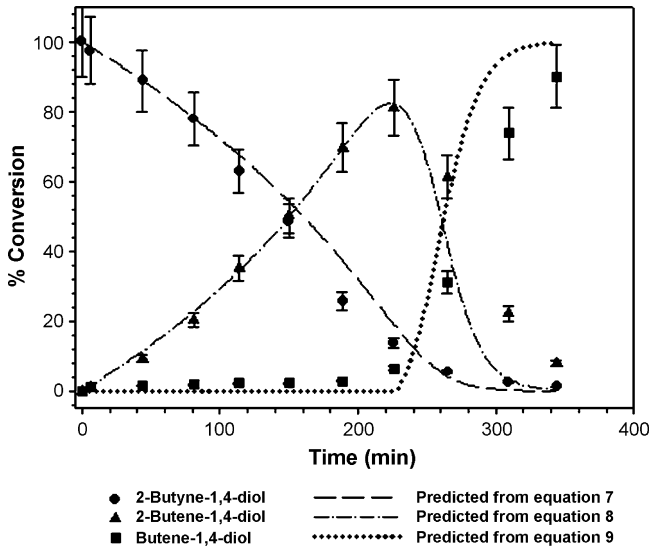

Fig. 3. Concentration profiles of 2-butyne-, 2-butene, and butane-1,4-diols as a function of time. Lines shown indicate model calculations from Eqs. (1)–(5) and (7) and (8). $V_{GS} = 0.013$ m s^{-1} and $V_{SL} = 0.067$ m s^{-1}.

The effect of competitive adsorption, which can cause negative orders in hydrogenation of olefins has been previously reported [35]. In hydrogenation over noble Group VIII metals, such as palladium and platinum, an adjacent–adsorption mechanism usually operates. 2-Butyne-1,4-diol hydrogenation proceeds through the adsorption of 2-butyne-1,4-diol and hydrogen on adjacent sites, followed by the reaction then desorption of 2-butene-1,4-diol as product. However, the negative order with respect to concentration of 2-butyne-1,4-diol might indicate that 2-butyne-1,4-diol is much more strongly adsorbed than hydrogen over palladium. The increase of 2-butyne-1,4-diol concentration resulted in increasing coverage of catalyst surface by 2-butyne-1,4-diol and therefore a reduction in the concentration of dissociated hydrogen on the active sites. As a result, the reaction rate decreased with increasing the 2-butyne-1,4-diol concentration.

The effects of changing the gas bubble and liquid slug lengths on the initial reaction rate are illustrated in Figs. 4 and 5. Fig. 4a shows the effect of dimensionless liquid slug length (L_S/D) upon the initial reaction rate as V_{SL} increased from 0.0074 to 0.1485 m s^{-1}, at constant V_{SG} = 0.0145 m s^{-1}. Increasing V_{SL} led to an increase in L_S/D; as shown in Fig. 4a. For short slugs with $L_S/D < 1$ the dependence of initial reaction rate upon L_S/D

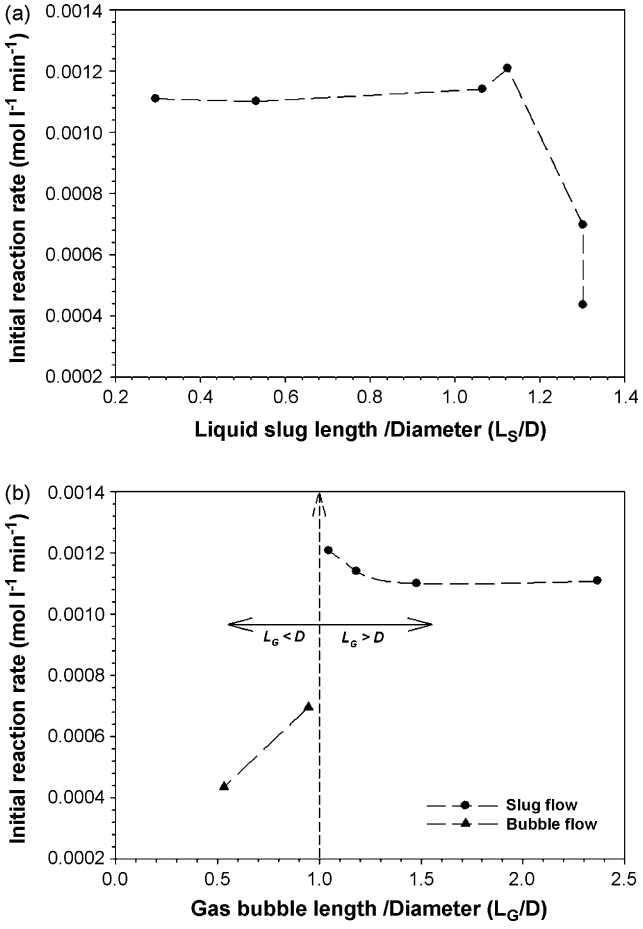

Fig. 4. Initial reaction rate at constant V_{SG} = 0.0145 m s^{-1} and increasing V_{SL} from 0.0074 to 0.1485 m s^{-1} vs. (a) L_S/D and (b) L_G/D. Lines are shown to guide the eye. Data shown correspond to the conditions in experiments 1–6 of Table 1.

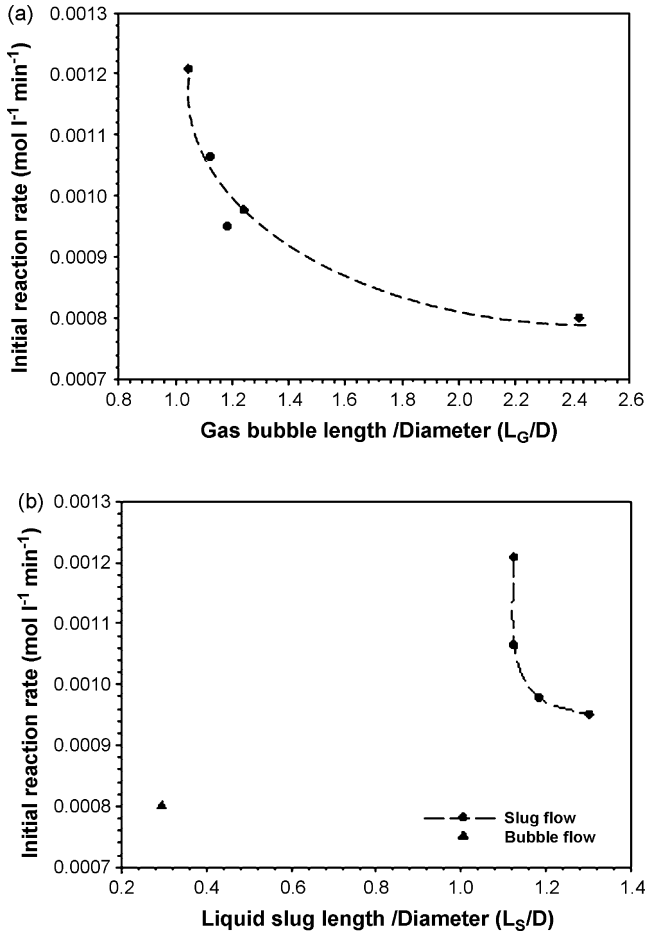

Fig. 5. Initial reaction rate at constant V_{SL} = 0.0743 m s^{-1} and increasing V_{SG} from 0.098 to 0.0359 m s^{-1} vs. (a) L_S/D and (b) L_G/D. Lines are shown to guide the eye. Data shown correspond to the conditions in experiments 7–10 of Table 1.

is small and remained at a value of 0.0011 mol l^{-1} min^{-1}. Upon further increase of V_{SL} the reaction rate increased slightly and reached a maximum of 0.0012 mol l^{-1} min^{-1} at $L_S/D \sim 1.2$. A similar optimum reaction condition was found $L_S/D \sim 1.7$ for NBA hydrogenation in a capillary [17]. The increase in initial reaction rate for values of L_S/D greater than unity might be attributed to changes in the velocity profiles previously observed by the authors between short ($L_S < D$) and long slugs ($L_S > D$) [36]. For short slugs, the profile of the axial velocity component across the capillary diameter was found to be flat resulting in the absence of a recirculation vortex, which in this case can explain the poor mass transfer when $L_S < D$. In the case of long slugs the profile was parabolic with the streamlines bending sharply around the end and the nose of the gas bubble and become straighter towards the walls of the capillary, thus giving rise to a recirculating flow which can enhance the mass transfer of hydrogen dissolved at the gas bubble interface by transporting it to the walls of the capillary. With further increase of V_{SL} beyond 0.111 m s^{-1}, such that $L_S/D > 1.2$, the reaction rate decreased dramatically since at the same time L_G decreased and Taylor flow ceased to exist due to the appearance of the bubbly flow pattern. For the reaction performed with NBA [17], the bubbly flow pattern was not

observed to appear until $L_S/D > 1.7$; this may explain the difference in optimum conditions. The interfacial tension of the liquid phases for NBA dissolved in propanol was 0.022 Nm^{-1}, compared with 0.0275 Nm^{-1} for the mixture used here. Under the bubbly flow regime the thin film between the bubble and the capillary wall is lost, and hence the film mass transfer step (i) disappears: the corresponding reduction in reaction rate illustrates the importance of film mass transfer upon the overall reaction rate.

Fig. 4b illustrates the effect of L_G/D upon the initial reaction rate under the same gas and liquid flows reported in Fig. 4a. For the region where $L_G/D > 1$ (circular points), the reaction rate decreased slightly with increasing L_G/D from an initial value of 0.0012 mol l^{-1} min^{-1} at $L_G \approx D$ and reached a constant value of 0.0011 mol l^{-1} min^{-1} for $L_G/D > 1.5$. As L_G is progressively increased, the fraction of the tube occupied by liquid is reduced, and therefore the contact time between the liquid and the catalyst is also reduced. The reduced liquid residence time could offset the effect of increased hydrogen mass transfer due to larger interfacial area of the thin film beside the gas slug, leading the weak influence of L_G upon reaction rate observed. Similarly from previous experiments [22], it was found that for the conversion of nitrite ions to nitrate ions (at constant L_S) L_G had only a weak influence on both mass transfer and reaction rate. For $L_G/D < 1$ (triangular points), the bubbly flow pattern occurs and the thin film surrounding the bubble is lost: the reaction rate is 42–63% lower than the maximum rate obtained for Taylor flow. This illustrates that the thin film of liquid at the side of the gas bubble does play an important role in hydrogen mass transfer; other studies have reported that mass transfer of hydrogen across the liquid film contributes 60–80% of the total gas to liquid mass transfer [30].

Fig. 5a and b show the effect of L_G/D and L_S/D, respectively upon the initial reaction rate as V_{SG} is increased from 0.098 to 0.0359 m s^{-1} at constant V_{SL} = 0.0743 m s^{-1}. Fig. 5a shows a general decrease in the initial reaction rate with increasing L_G/D. The trend is similar to Fig. 4b although the rate of decrease is somewhat higher. Again, although increasing the gas slug length increases the surface area of the thin film around the gas bubble, the hold up of liquid in the tube and hence the liquid contact time is reduced, leading to a consequent reduction in reaction rate.

Fig. 5b shows for $L_S/D > 1.1$ in the Taylor flow regime that the reaction rate decreased by 20% as L_S/D increased between 1.1 and 1.3. Horvath et al. [18] measured the radial mass transfer in slug flow regime in a circular channel with immobilized enzyme on the inner wall and observed a rapid decrease in mass transfer by 30% with an increase of L_S/D from 1 to 2.5 and a further decrease of 10% between $2.5 < L_S$ and $D < 5$. They observed no further effect upon mass transfer above $L_S/D > 5$. For slugs with $L_S > D$, increasing the liquid slug length leads to an increase in the mass transfer distance from the gas–liquid interface at the bubble nose to the liquid slug and then to the catalyst wall. Thus the reaction rate decreases for longer liquid slugs. Similarly, for short slugs, $L_S < D$, the reaction rate has decreased dramatically due to undeveloped liquid profile and lack of internal recirculation [36]. For bubbly flow (Fig. 5b, triangular point), the reaction rate is lower as observed in Fig. 4.

In summary, from Fig. 4 at constant V_{SG}, the initial reaction rate is a strong function of flow pattern with a strong dependence on L_S and weak dependence on L_G in the Taylor flow regime. However at constant V_{SL}, it is shown in Fig. 5 that the initial reaction rate is equally sensitive to both parameters.

4.2. Kinetic studies

The temperature dependence of the reaction rate was investigated between temperatures of 24 and 50 °C at constant gas and liquid superficial velocities of V_{SG} = 0.0118 m s^{-1} and V_{SL} = 0.0594 m s^{-1}. An Arrhenius plot is shown in Fig. 6, where the straight line represents the best fit to the experimental data; the calculated value of apparent activation energy was 9.05 kJ mol^{-1}. Previous studies of the same reaction in a capillary reactor operated under Taylor flow led to the determination of an apparent activation energy of 33 kJ mol^{-1}, 1, where the mass transport resistances were concluded to be negligible [32]. However, in this study, the much lower value of activation energy determined suggests that the reaction is mass transfer limited.

In order to model the reaction rates, the kinetic models described by Eqs. (7) and (8) were combined with the mass transfer relationships given by Eqs. (1)–(5). In order to utilise the kinetic model, it was necessary to fit the kinetic parameters of Eqs. (7) and (8), namely k_r, K_H, K_{B3}, and k_{B2} to the experimental data.

The influence of initial 2-butyne-1,4-diol concentration on the rate was studied at temperature of 24 °C, at atmospheric pressure for the initial concentrations of 0.1 to 0.52 mol l^{-1}. Fig. 7 shows that the reaction rate was restricted by the amount of 2-butyne-1,4-diol in the solution, again suggesting that the greater affinity of the active catalyst sites for 2-butyne-1,4-diol than hydrogen, leads to a reduction in the reaction rate when 2-butyne-1,4-diol is in excess. If a power law model is assumed an order of −0.8 towards 2-butyne-1,4-diol is found in this work. Data from previous studies [37] gave an approximate order of −0.2 in butyne-1,4-diol over $Pd/CaCO_3$ at 15 °C, and later

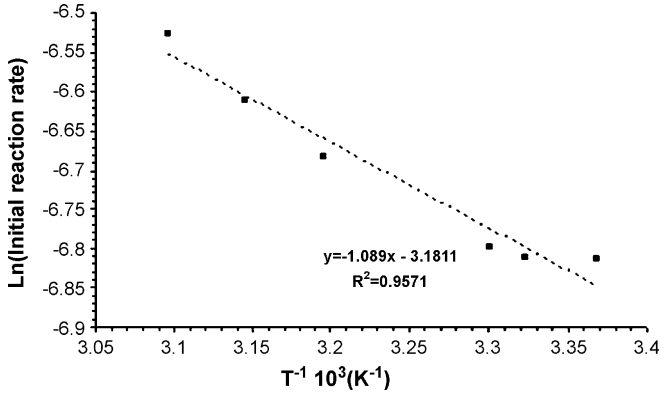

Fig. 6. Arrhenius plot for 2-butyne-1,4-diol hydrogenation. Data shown correspond to the conditions in experiments 11–16 of Table 1.

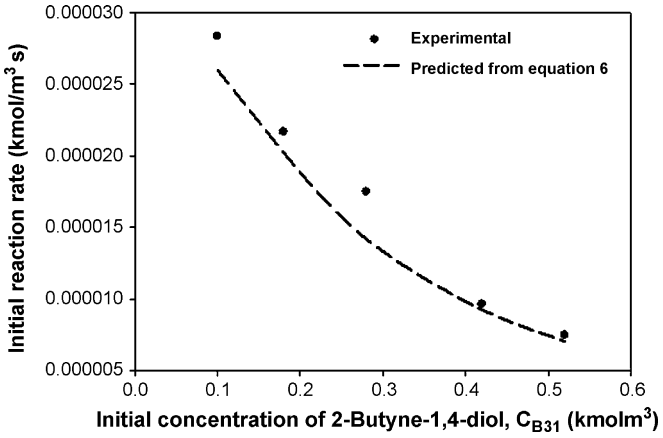

Fig. 7. Initial reaction rate vs. initial concentration of 2-Butyne-1,4-diol. The line indicates model calculations from Eq. (6). Data shown correspond to the conditions in experiments 17–21 of Table 1.

Chaudhari [34] used 0.2% Pd/C and obtained a higher negative order of −1.4 at 40 °C. Most workers found that the order was negative, however a zero order has been reported [38] using a Raney nickel catalyst, which is a less active catalyst compared with palladium.

The parameters from Eq. (6), k_r, K_H, and K_{B3}, were estimated via a non-linear least square regression analysis, for which the sum of the squares (SSR) of the difference between the observed and predicted rates was minimised. Eq. (6) was fitted to the experiment given in Table 2 and the results are shown in Fig. 7. An enhancement of the ratio K_H/K_{B3} from 0.0015 [32] to 0.087 (current study) is observed when the hydrogenation is carried out under different flow conditions. The strong adsorption of 2-butyne-1,4-diol compared with hydrogen has been previously observed [32] where K_H was 0.00128–0.079 times lower than K_{B3} for a Pd/Al_2O_3 monolith reactor operated with increasing gas hold up from 0.33 to 0.7. Similarly for the same catalyst it was found [15] that K_H was 0.43 and 0.079 and 0.85 times lower than K_{B3} for a slurry and monolith reactor, respectively.

Eqs. (7)–(9) were used for the estimation of 2-butyne-1,4-diol, 2-butene-1,4-diol and butane-1,4-diol concentration and the results are shown in Fig. 3. Using a similar approach to this work, hydrogen mass transport equations have been previously combined with a Langmuir–Hinshelwood rate equation [5] to describe the reaction performance of styrene hydrogenation over palladium on alumina catalyst. The lines on Fig. 3 show the model predictions of this work, illustrating that the reduction of 2-butyne-1,4-diol at high concentrations (>50%) is predicted quite well but then the model and under predicts the experimental values at lower concentrations. At low 2-butyne-1,4-diol concentrations towards the end of the reaction, the rate is limited by the diminished concentration of 2-butyne-1,4-diol in solution rather than hydrogen mass transport which is assumed in the model equations. Similar results were observed for the hydrogenation of NBA [39]; it was found that the rate of hydrogen mass transfer controls the reaction for an initial concentration of 0.02 mol l^{-1} and at lower concentration of 0.0005 mol l^{-1} the reaction is limited by the remaining concentration of NBA in solution. The model performs similarly for the concentration of 2-butene-1,4-diol in that it gives a good prediction at high concentrations and under estimates at lower concentrations, when less than 10% of the starting concentration of 2-butyne-1,4-diol remains in solution. Once the concentration of 2-butyne-1,4-diol decreases below 10%, the value of the inhibiting term for R_{B2} decreases in Eq. (8), such that the rate strongly accelerates. A possible improvement in the model fit would be to include a term $K_{B2}C_{B2}$ in the denominator of the L–H model for R_{B2} within Eq. (8). However, for the purposes of this work, the uncertainty of including an extra fitted parameter was not deemed to be advantageous.

Table 2
Modelling results for fitting kinetic model a representative set of experiments

Parameter	Optimal estimate	Sum of the squares, SSR
k_r (kmol m^{-3} s^{-1})	0.38	5.3×10^{-11}
K_H (m^3 $kmol^{-1}$)	0.66	
K_{B3} (m^3 $kmol^{-1}$)	7.55	
k_{B2} (kmol m^{-3} s^{-1})	0.06	

4.3. Effect of hydrodynamics on selectivity

The selectivity towards *cis*-butenediol is defined as the ratio of the moles of *cis*-butene-1,4-diol produced to the moles of 2-butyne-1,4-diol converted to products. The operating aspects investigated in connection with the selectivity are the effects of gas and liquid flow rate, initial concentration and temperature. Additives are sometimes required to improve the selectivity towards a desired product, however in any industrial process, these must then be removed afterwards which means the process requires an additive recovery stage at additional cost. The selectivity investigation in the capillary reactor was carried out without additives, since it would be of great advantage if high selectivity can be reached in this manner.

Fig. 8 shows a typical trend of selectivity versus conversion of 2-butyne-1,4-diol during the capillary reaction for the

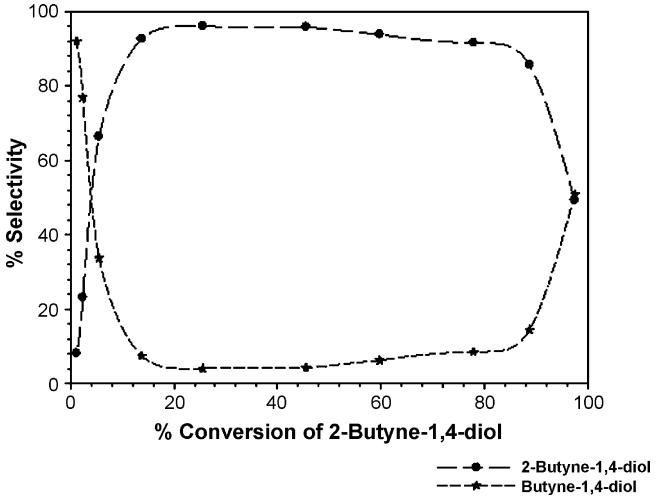

Fig. 8. Selectivity towards 2-butene-1,4-diol and butane-1,4-diol vs. conversion of 2-butyne-1,4-diol for V_{GS} = 0.013 m s^{-1} and V_{SL} = 0.067 m s^{-1}.

same reaction conditions as shown in Fig. 3, namely $V_{GS} = 0.013$ m s^{-1} and $V_{SL} = 0.067$ m s^{-1}. Generally, the trend shows that the selectivity was very high at conversions within the range of 15–77%. Within this range, a very strong adsorption of acetylenic compound compared to olefin occurred [35]. Beyond 77% conversion, the concentration of 2-butyne-1,4-diol decreased significantly, allowing adsorption of the olefin. Above this point, the selectivity towards 2-butene-1,4-diol decreased rapidly with the solution containing butane-1,4-diol as end product.

The influence of flow rate upon selectivity was investigated at constant $V_{SG} = 0.0145$ m s^{-1} whilst varying V_{SL} (Fig. 9a) and at constant $V_{SL} = 0.0743$ m s^{-1} whilst varying V_{SG} (Fig. 9b). The investigation was carried out at 24 °C with a concentration of 0.28 mol l^{-1} 2-butyne-1,4-diol. Fig. 9a shows that the selectivity to 2-butene-1,4-diol is sensitive to increasing V_{SL} from 0.0074 to 0.1485 m s^{-1} at constant $V_{SG} = 0.0145$ m s^{-1}, experiments 1–6 from Table 1. In this work the selectivity ranged from 20–90%, at 90% conversion of 2-butyne-1,4-diol. However, it was found previously that high selectivity values towards the 2-butene-1,4-diol occur in both

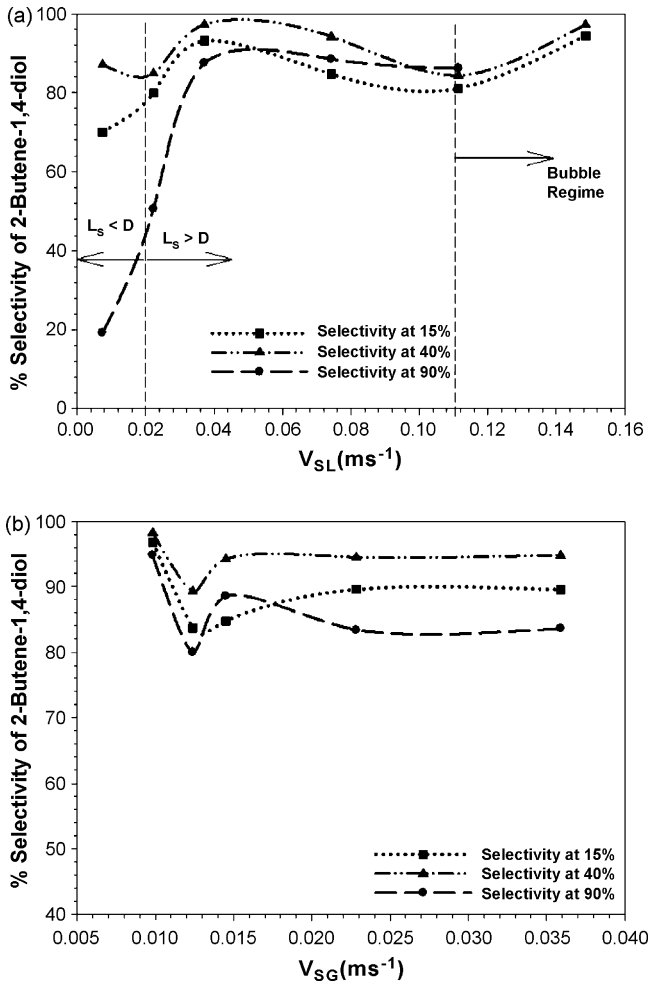

Fig. 9. Selectivity vs. (a) increasing V_{SL} and (b) increasing V_{SG}. Data shown correspond to the conditions in experiments 4 and 7–10 of Table 1. The legends of Figs. 9–11 indicate the percentage conversion of 2-butyne-1,4-diol at which the selectivity to 2-butene-1,4-diol was measured.

the single capillary and monolith reactor at 100% conversion of alkyne at a single gas and liquid flow rate [32]. In their work a different catalyst was used to the present study, which may have led to the higher selectivity values observed. Fig. 9a indicates that for $V_{SL} = 0.0372$ m s^{-1} a maximum in selectivity occurred.

At 15% conversion the selectivity increases from 70 to 84.7% with increase of V_{SL} from 0.0074 to 0.0372 m s^{-1} (corresponding to an increase in L_S). Recirculation patterns inside the liquid start to appear for $L_S > D$ and enhance the mass transfer from the gas bubble to the liquid slug and then to the catalyst surface. In this case, 2-butyne-1,4-diol replaces desorbed 2-butene-1,4-diol due to its high adsorption rate, thus avoiding further 2-butene-1,4-diol conversion and the selectivity increases. Similarly with 40 and 90% conversion, at 15% conversion further increase of the V_{SL} beyond 0.0372 m s^{-1} causes the selectivity to decrease slightly to 81%.

When the conversion was 40%, however, there is no significant influence of V_{SL} on selectivity for the case of $L_S < D$. When the value of V_{SL} was increased above 0.021 m s^{-1} the selectivity increased from 85% up to 97.3% at 0.0372 m s^{-1} and decreased to 85.7% with further increase of the flow to 0.112 m s^{-1}. The decrease in the selectivity towards 2-butene-1,4-diol with increasing the liquid velocity was also observed previously in a trickle bed reactor operated under plug flow [33]. They found that selectivity decreased by 9% with doubling the liquid velocity for the same mixed solvent, 30% (v/v) isopropanol–water.

Fig. 9a clearly indicates that at 90% conversion, the selectivity significantly depends on the liquid flow rate and flow pattern. It seems at low $V_{SL} = 0.0074$ m s^{-1} where $L_S < D$ the selectivity is low. As the V_{SL} is increased to the point where $L_S = D$, the selectivity increases from 19.4 to 50.7%. Further increase of the V_{SL} such that $L_S > D$ leads to an increase in selectivity to 91.4%. As discussed earlier, for $L_S > D$ mass transport is enhanced by recirculation patterns that occur in the liquid slug [36]. The selectivity at 90% conversion is lower than at 40% conversion and this can be explained by in terms of adsorption energies [35]. 2-Butyne-1,4-diol is strongly adsorbed relative to 2-butene-1,4-diol that it dominates the surface, as long as there is a good 2-butyne-1,4-diol surface coverage, 2-butene-1,4-diol is not hydrogenated. On the other hand a lower alkyne diol surface concentration allows the olefin to completely adsorbed on the surface. At this stage the 2-butyne-1,4-diol coverage is decreased and 2-butene-1,4-diol is also adsorbed on the metal site; thereby the 2-butene-1,4-diol hydrogenation takes place resulting in a drop in the overall selectivity.

By comparing the selectivities obtained in slug flow regimes with bubble regime, it is observed that the highest selectivity, a range of 94–97% occurs in the bubble flow regime. However, these high selectivities were reached for 15 and 40% conversion of 2-butyne-1,4-diol, as 90% conversion was not reached due to the very slow reaction rate.

The selectivity observed at a value of constant $V_{SL} = 0.0074$ m s^{-1} and increasing V_{SG} from 0.098 to 0.0359 m s^{-1} is shown in Fig. 9b. The trend shown indicates a slight decrease of selectivity with increasing V_{SG} from 0.098 to 0.0124 m s^{-1} while a steady value is reached at higher gas flow rates.

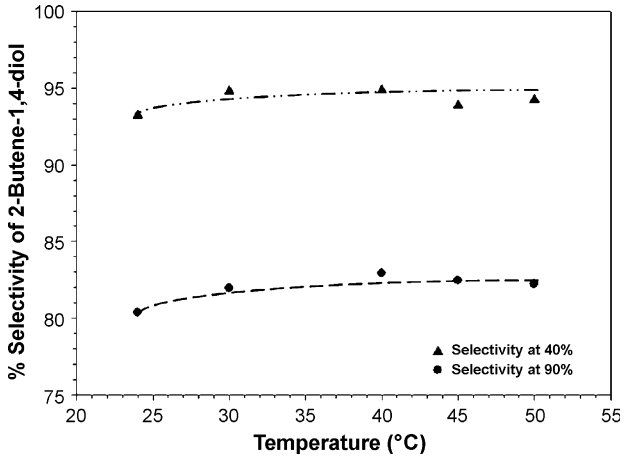

Fig. 10. Effect of temperature on selectivity.

The temperature dependence of the selectivity was investigated at temperatures of 24–50 °C at constant $V_{SG} = 0.0118$ and $V_{SL} = 0.059$ m s^{-1}. Fig. 10 indicates that the selectivity decreased slightly with increasing the temperature and then tended to a constant value at higher temperatures. At higher temperatures, diffusivity of hydrogen in the solvent increases, which could lead to increased mass transfer rates. However, the increase in temperature can also lower the hydrogen solubility in the liquid, and may affect differently the rates coefficients of the two hydrogenation steps depending on their activation energies. Therefore, the effect of temperature upon the selectivity towards 2-butene-1,4-diol is quite complex.

The effect of initial concentration of 2-butyne-1,4-diol as substrate was also investigated in the range of 0.1 to 0.52 mol l^{-1} at a temperature 24 °C, $V_{SG} = 0.0118$ m s^{-1} and $V_{SL} = 0.0594$ m s^{-1}. Fig. 11 shows that the initial concentration of 2-butyne-1,4-diol did not influence the magnitude of the selectivity for 15 and 40% conversion. At these conversions, the selectivity towards 2-butene-1,4-diol was observed to lie in the range of 93 to 97%. However, at 90% conversion selectivity is significantly lower than at 15% or 40% conversion. Upon increasing the initial concentration of 2-butyne-1,4-diol from 0.1 to 0.52 mol l^{-1} the selectivity increases from 9.6 to 97%. The reason for this is again the competitive adsorption between 2-butyne-1,4-diol and 2-butene-1,4-diol, whereupon at lower concentrations of 2-butyne-1,4-diol the 2-butene-1,4-diol is able to adsorb on the catalyst. This leads to a greater production of the butane-1,4-diol.

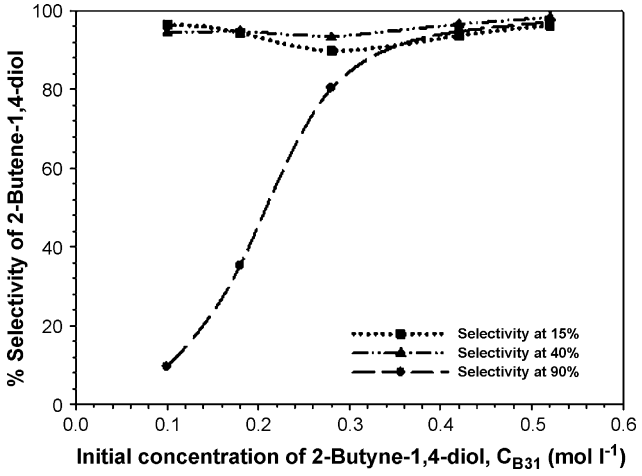

Fig. 11. Effect of initial 2-butyne-1,4-diol concentration on selectivity.

5. Conclusions

The influence of two-phase flow hydrodynamics on initial reaction rate and selectivity in vertical capillary with circular diameter were experimentally studied using the hydrogenation of 2-butyne-1,4-diol as a model reaction. It was demonstrated that the reaction rate under Taylor flow was higher than that of bubble flow, with two distinct cases of $L_S < D$ and $L_S > D$. At constant V_{SG} the reaction rate reached a maximum of 0.0012 mol l^{-1} min^{-1} for long liquid slugs at $L_S/D \sim 1.2$. Within the Taylor flow regime at constant V_{SL} and increasing V_{SG}, with $L_G/D \sim 1.5$, the reaction rate reached a steady value of 0.0011 mol l^{-1} min^{-1}. Finally in the bubble flow regime the reaction rate decreased to 0.0008 mol l^{-1} min^{-1}. At constant V_{SL} the reaction rate decreased with increasing L_i and L_G. Using kinetic and mass transfer expressions from literature a model for the hydrogenation of 2-butyne-1,4-diol was developed with excellent agreement in the hydrogen mass transfer limited regime, but poorer prediction at the end of the reaction when the 2-butyne-1,4-diol concentration limits the reaction. The selectivity towards the desired product, 2-butene-1,4-diol was found to be a function of V_{SL} (at constant V_{SG}) for the two distinctive cases of $L_S > D$ and $L_S < D$ and reached a maximum value of 97.3% at moderate velocities $V_{SL} = 0.037$ and $V_{SG} = 0.0145$ m s^{-1}.

References

[1] A. Cybulski, A. Stankiewicz, R.K. Edvinnsson Albers, J.A. Moulijn, Chem. Eng. Sci. 54 (1999) 2351.
[2] R.K. Edvinsson, A. Cybulski, Catal. Today 24 (1995) 173.
[3] T.A. Nijhuis, M.T. Kreutzer, A.C.J. Romijn, F. Kapteijn, J.A. Moulijn, Chem. Eng. Sci. 56 (2001) 823.
[4] T.A. Nijhuis, M.T. Kreutzer, A.C.J. Romijn, F. Kapteijn, J.A. Moulijn, Catal. Today 66 (2001) 157.
[5] T.A. Nijhuis, F.M. Dautzenberg, J.A. Moulijn, Chem. Eng. Sci. 58 (2003) 1113.
[6] R. Kulkarni, R. Natividad, J. Wood, E.H. Stitt, J.M. Winterbottom, Catal. Today 105 (2005) 455.
[7] S. Irandoust, B. Andersson, E. Bengtsson, M. Siverstroem, Ind. Eng. Chem. Res. 28 (1989) 1489.
[8] R. Edvinsson Albers, M. Nystrom, M. Siverstrom, A. Sellin, A.C. Dellve, U. Andersson, W. Herrmann, T. Berglin, Catal. Today 69 (2001) 247.
[9] M.D. Mantle, A.J. Sederman, L.F. Gladden, S. Raymahasay, J.M. Winterbottom, E.H. Stitt, AICHE 48 (2002) 909.
[10] M.T. Kreutzer, M.G. Eijnden, F. Kapteijn, J.A. Moulijn, J.J. Heiszwolf, Catal. Today 105 (2005) 667.
[11] M.T. Kreutzer, J.J.W. Bakker, F. Kapteijn, J.A. Moulijn, P.J.T. Verheijen, Ind. Eng. Chem. Res. 44 (2005) 4898.
[12] M.T. Kreutzer, P. Du, J.J. Heiswolf, F. Kapteijn, J.A. Moulijn, Chem. Eng. Sci. 56 (2001) 6015.
[13] I. Ochuma, R.P. Fishwick, J. Wood, J.M. Winterbottom, Appl. Catal. B 73 (2007) 259.

[14] X. Quan, H. Shi, Y. Zhang, J. Wang, Q. Yi, Process Biochem. 38 (2003) 1545.
[15] H. Marwan, J.M. Winterbottom, Catal. Today 97 (2004) 325.
[16] J.M. Winterbottom, H. Marwan, J. Viladevall, S. Sharma, S. Raymahasay, Stud. Surf. Sci. Catal. 108 (1997) 59.
[17] A.N. Tsoligkas, M.J.H. Simmons , J. Wood, Chem. Eng. Sci., in press, doi:10.1016/j.ces.2006.11.022.
[18] C. Horvath, B.A. Solomon, J.M. Engasser, Ind. Eng. Chem. Fund. 12 (1973) 431.
[19] D.R. Oliver, S.J. Wright, Br. Chem. Eng. 9 (1964) 590.
[20] T.C. Thulasidas, M.A. Abraham, R.L. Cerro, Chem. Eng. Sci. 52 (1997) 2947.
[21] T.C. Thulasidas, M.A. Abraham, R.L. Cerro, Chem. Eng. Sci. 54 (1999) 61.
[22] G. Berčič, A. Pintar, Chem. Eng. Sci. 52 (1997) 3709.
[23] L. Chen, Y.S. Tian, T.G. Karayiannis, Int. J. Heat Mass Transfer 49 (2006) 4220.
[24] T. Furukawa, T. Fukano, Int. J. Multiphase Flow 27 (2001) 1109.
[25] F. Dong, X. Liu, X. Deng, L. Xu, L. Lu, Meas. Sci. Technol. 12 (2001) 1069.
[26] G.I. Taylor, J. Fluid Mech. 10 (1961) 161.
[27] T. Bauer, R. Guettel, S. Roy, M. Schubert, M. Al-Dahhan, Lange, Chem. Eng. Res. Des. 83 (2005) 811.
[28] S. Irandoust, B. Andersson, Ind. Eng. Chem. Res. 28 (1989) 1684.
[29] C.R. Wilke, P. Chang, AICHE J 264 (1955) 264.
[30] J.M. Baten, R. Krishna, Chem. Eng. Sci. 59 (2004) 2534.
[31] L.G. Nishchenkova, M.V. Ulitin, V.N. Gorelov, Khimiya i Khimicheskaya Tekhnologiya 33 (1990) 22.
[32] R. Natividad, R. Kulkarni, K. Nuithitikul, S. Raymahasay, J. Wood, J.M. Winterbottom, Chem. Eng. Sci. 59 (2004) 5431.
[33] J.M. Winterbottom, H. Marwan, E.H. Stitt, R. Natividad, Catal. Today 79–80 (2003) 391.
[34] R.V. Chaudhari, R. Jaganathan, E.D.S. Kolhe, H. Hofmann, Appl. Catal. A 29 (1987) 141.
[35] G.C. Bond, G. Webb, P.B. Wells, J.M. Winterbottom, J. Catal. 1 (1962) 74.
[36] A.N. Tsoligkas, M.J.H. Simmons, J. Wood, Chem. Eng. Sci. 62 (2007) 4365–4378.
[37] T. Fukuda, T. Kusama, Bull. Chem. Soc. Jpn. 31 (1958) 339.
[38] C. Rongfu, G. Qiwei, J. East China Inst. Chem. Tech. 14 (1988) 269.
[39] G. Berčič, Catal. Today 69 (2001) 147.